Electronic Supplementary Material (ESI) for Soft Matter.

Supporting Information

A Mixed Ligand Approach towards Lanthanide Based Gels Using Citric Acid as Assembler Ligand: White Light Emission and Environmental Sensing

*Alphy Sebastian, Malay Krishna Mahato, and Edamana Prasad**

Department of Chemistry,

Indian Institute of Technology Madras,

Chennai-600036, Tamil Nadu

India

Corresponding author email: pre@iitm.ac.in

Table of contents **Page**

1. Synthesis and characterizations of 4'-(4-bromophenyl)-2,2':6',2''-terpyridine

2-Acetyl pyridine (3 equivalents) was added to 120 mL methanol solution of 4-bromobenzaldehyde (1.0 g, 5.40 mmol), NaOH (0.22 g, 5.4 mmol) and 30 mL concentrated NH_4OH. The reaction mixture was refluxed for 2 days, and then let to reach room temperature. The formed slight yellow precipitate was filtered and washed sequentially with H_2O and cold CH_3OH. Recrystallization from ethanol yield 4'-(4-bromophenyl)-2,2':6',2"-terpyridine as white solid (1.8 g, 88% yield). ^{1}H NMR (400 MHz, $CDCl_3$) δ (ppm): 8.72 (d, 2H), 8.66 (s, 2H), 8.64 (d, 2H), 7.86 (m, 2H), 7.76 (d, 2H), 7.63 (d, 2H), 7.34 (m, 2H). ^{13}C NMR (100 MHz, $CDCl_3$) δ (ppm): 156.0, 149.1, 149.0, 137.4, 136.9, 132.1, 128.9, 123.9, 123.4, 121.3, 118.5

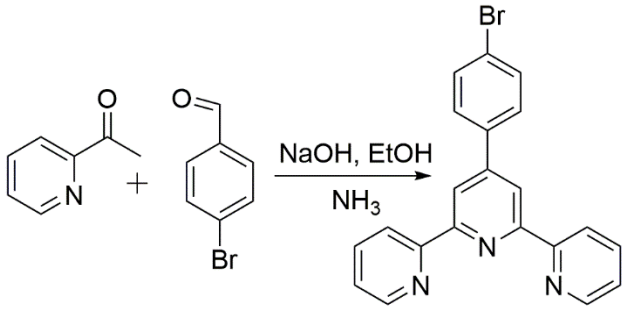

Scheme S1: Synthesis of compound 4'-(4-bromophenyl)-2,2':6',2"-terpyridine

^{1}H NMR

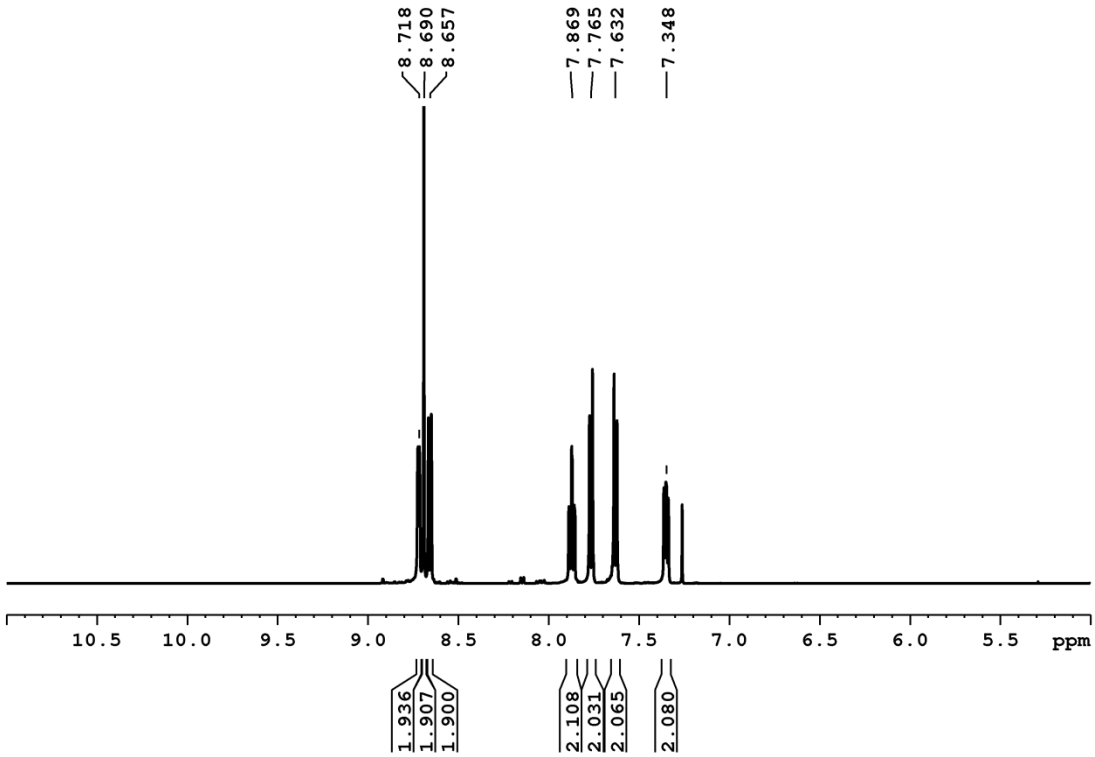

Figure S1: ^{1}H NMR spectrum of 4'-(4-bromophenyl)-2,2':6',2''-terpyridine

^{13}C NMR

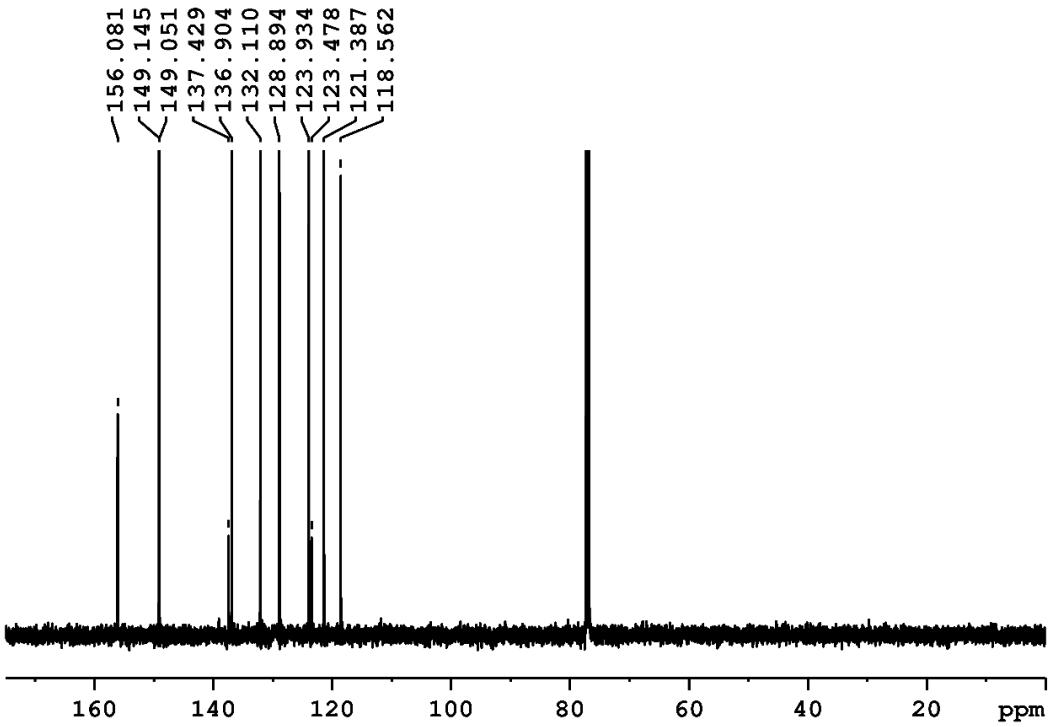

Figure S2: ^{13}C NMR spectrum of 4'-(4-bromophenyl)-2,2':6',2"-terpyridine

HRMS

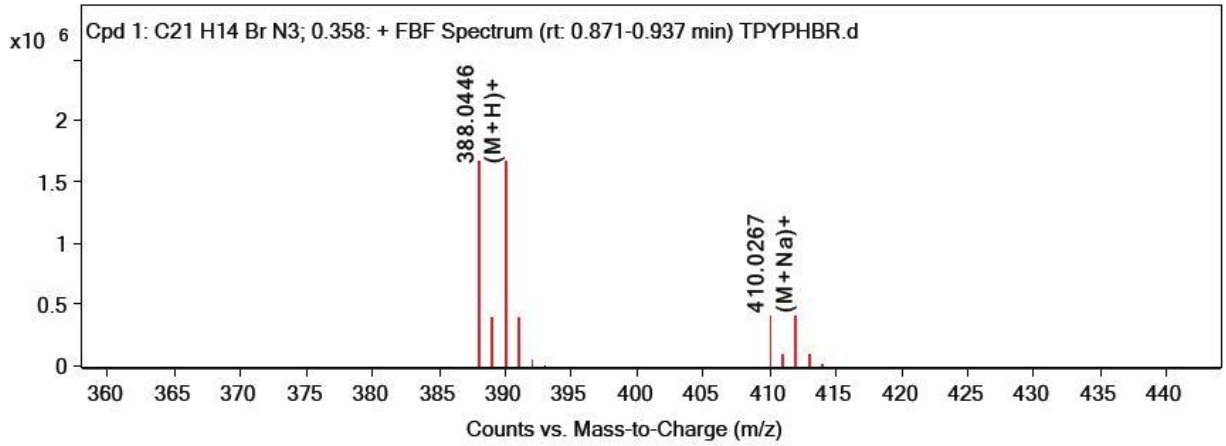

Figure S3: HRMS of 4'-(4-bromophenyl)-2,2':6',2"-terpyridine

2. Table S1 Containing details of gelation test

Gelation ability results of the bicomponent (citric acid anhydrous + Ln (III) acetate) system tested in various solvents, with known Kamlet-Taft parameters.

Entry	Solvent	Phase	Kamlet-Taft solvent parameters		
			α	β	π*
1	H_2O	S	1.17	0.47	1.09
2	DMSO	G	0.00	0.76	1.00
3	DMF	G	0.00	0.69	0.88
4	DMAc	G	0.00	0.76	0.88
5	NMP	G	0.00	0.77	0.92
6	CH_3CN	PS	0.19	0.40	0.79
7	THF	PG	0.00	0.55	0.58
8	MeOH	PG	0.98	0.66	0.60
9	EtOH	PG	0.86	0.75	0.54
10	EtOAc	I	0.00	0.45	0.55
11	CH_2Cl_2	I	0.13	0.10	0.82
12	Hexane	I	0.00	0.00	-0.04
13	Toluene	I	0.19	0.40	0.75
14	Benzene	I	0.00	0.10	0.59

S=Soluble, G=Gel, PS=Partially soluble, PG=Partial gel, I=Insoluble

3. SEM images of CA Eu and CA Tpy Eu xergels

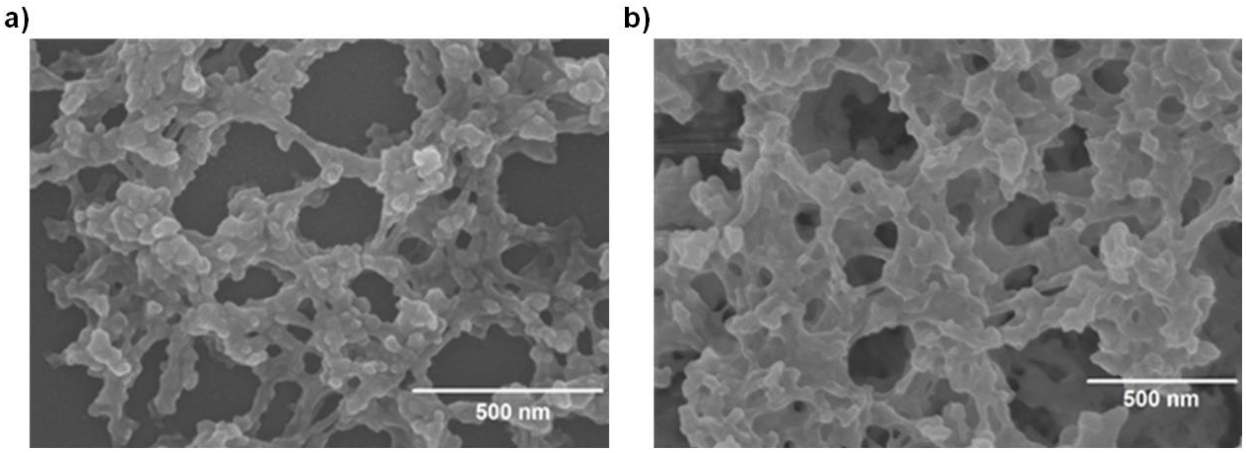

Figure S3: SEM images of a) CA Eu and b) CA Tpy Eu xerogels.

4. IR spectra of Tpy, CA Eu xerogel and CA Tpy Eu xerogel

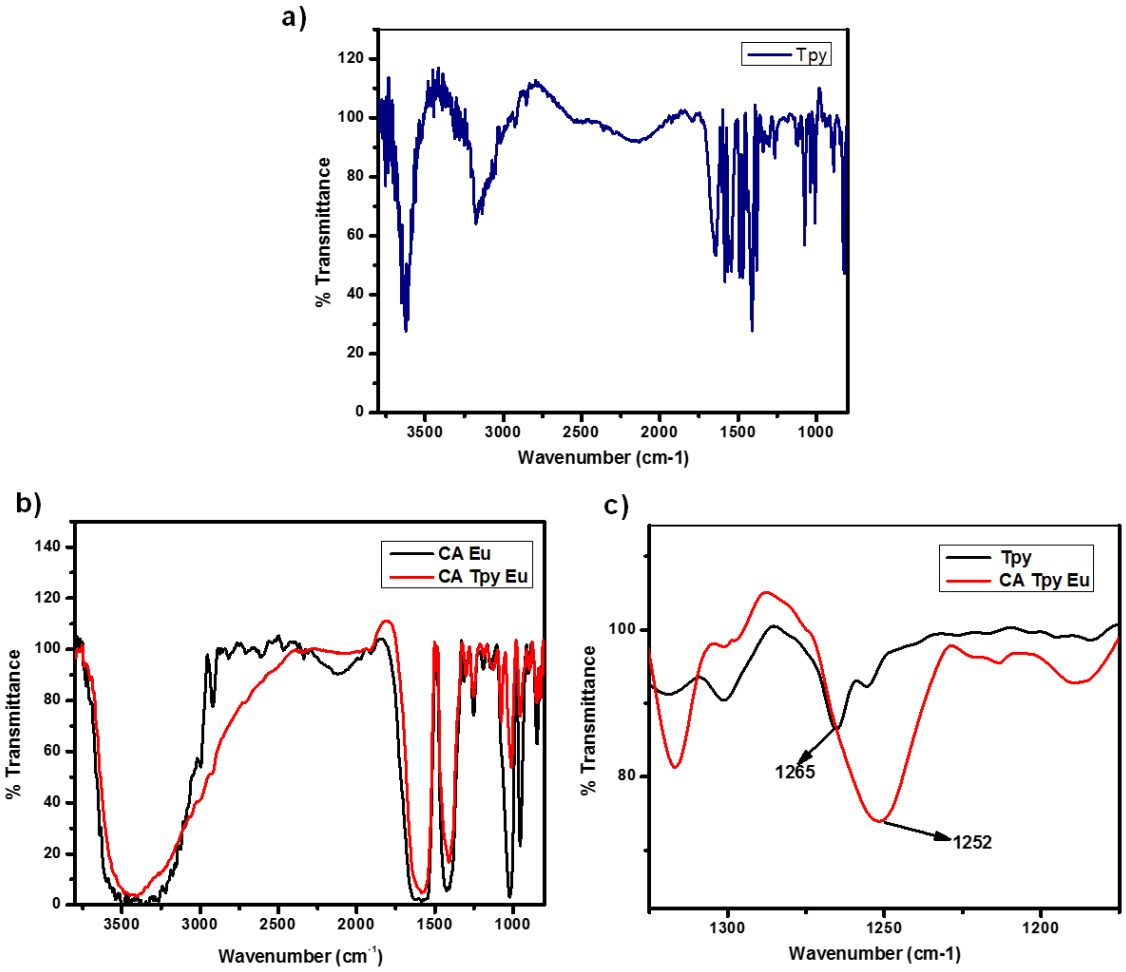

Figure S4: a) IR spectrum of Tpy.b) IR spectra of CA Eu (black line) and CA Tpy Eu (red line) xerogels.c) Zoomed IR spectra of Tpy (black line) and CA TpyEu (red line).

5. Elastic stress versus strain graph

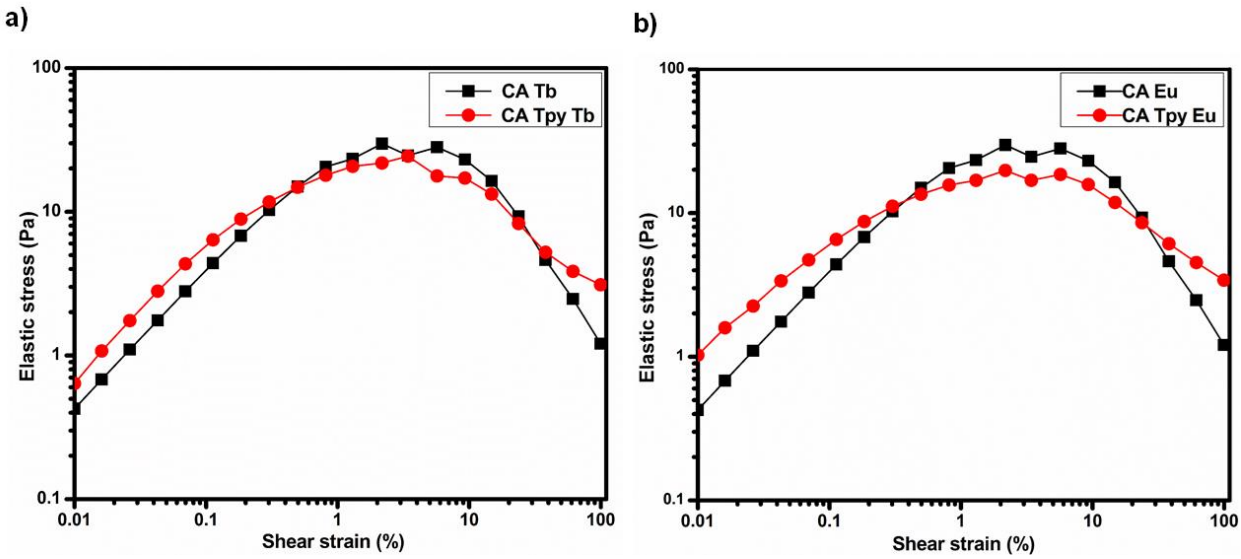

Figure S5: Elastic stress versus strain graph for a) CA Tb and CA Tpy Tb and b) CA Eu and CA Tpy Eu.

6. Strain sweep and Frequency sweep studies of CA Eu and CA Tpy Eu gels

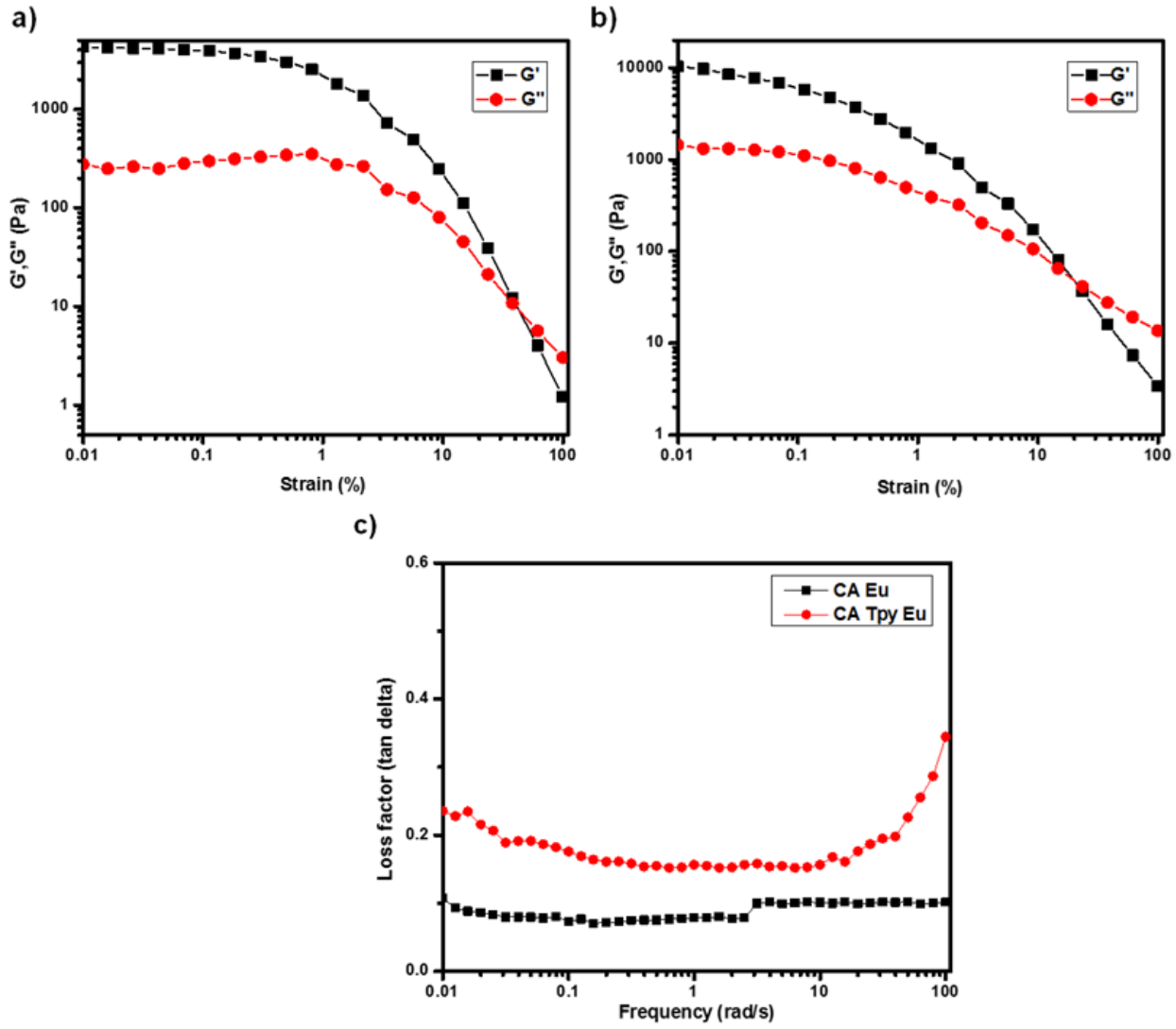

Figure S6: Strain sweep meassurements of a) CA Eu and b) CA Tpy Eu gels. c) tan delta vs. frequency sweep data of CA Eu and CA Tpy Eu gels.

7. MALDI spectrum for the CA Eu xerogel

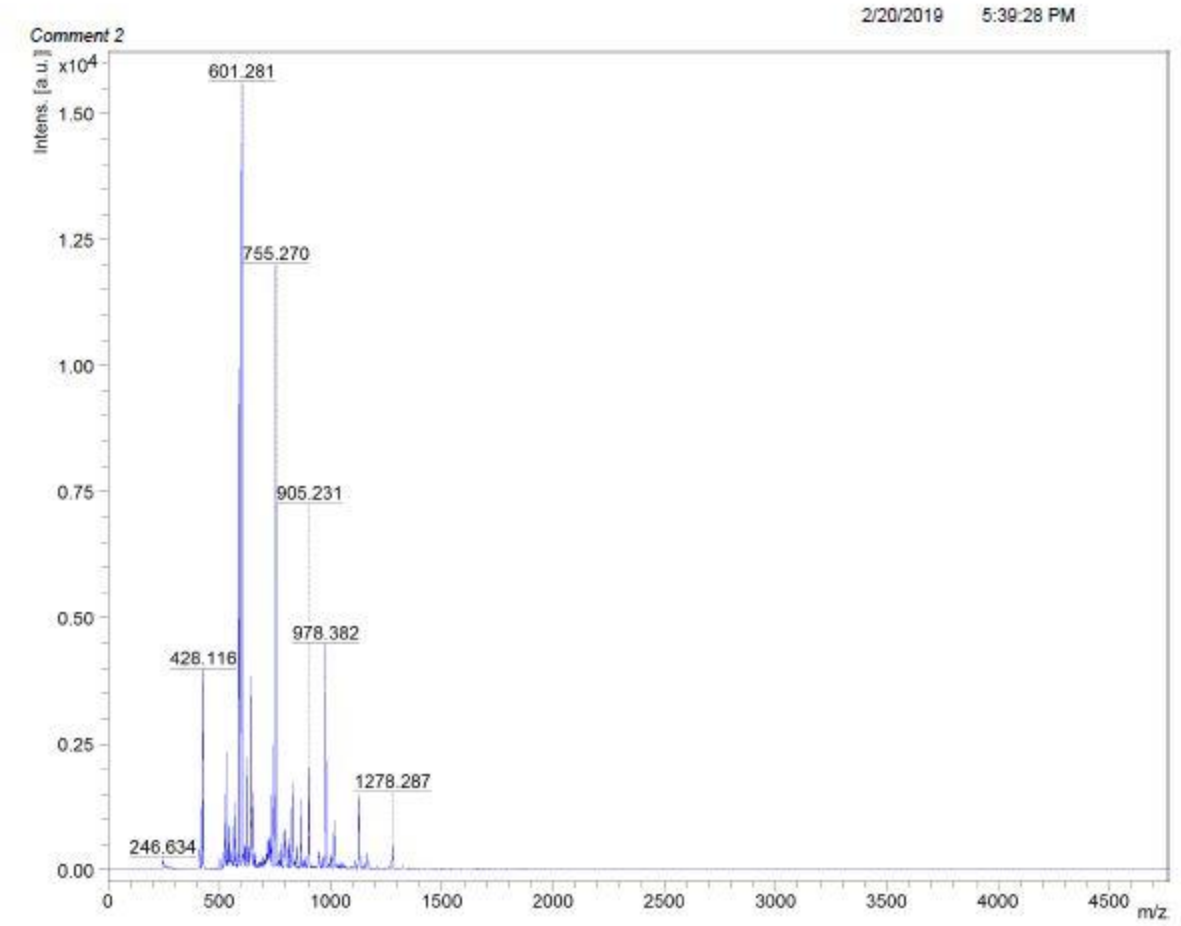

Figure S7: MALDI spectrum of CA Eu (1:1) xerogel in 30% methanolic water solution.

The highest m/z value of 1278 account for the formation of coordination oligomer with at least three Eu (III) centers. Higher oligomers are not observed in the MALDI spectrum because of the poor solubility of the higher oligomers (The xerogel was very poorly soluble in methanolic solution which is in agreement with the literature reports of lanthanide citrate coordination polymers).[1]

8. Comparison of ^{13}NMR spectra

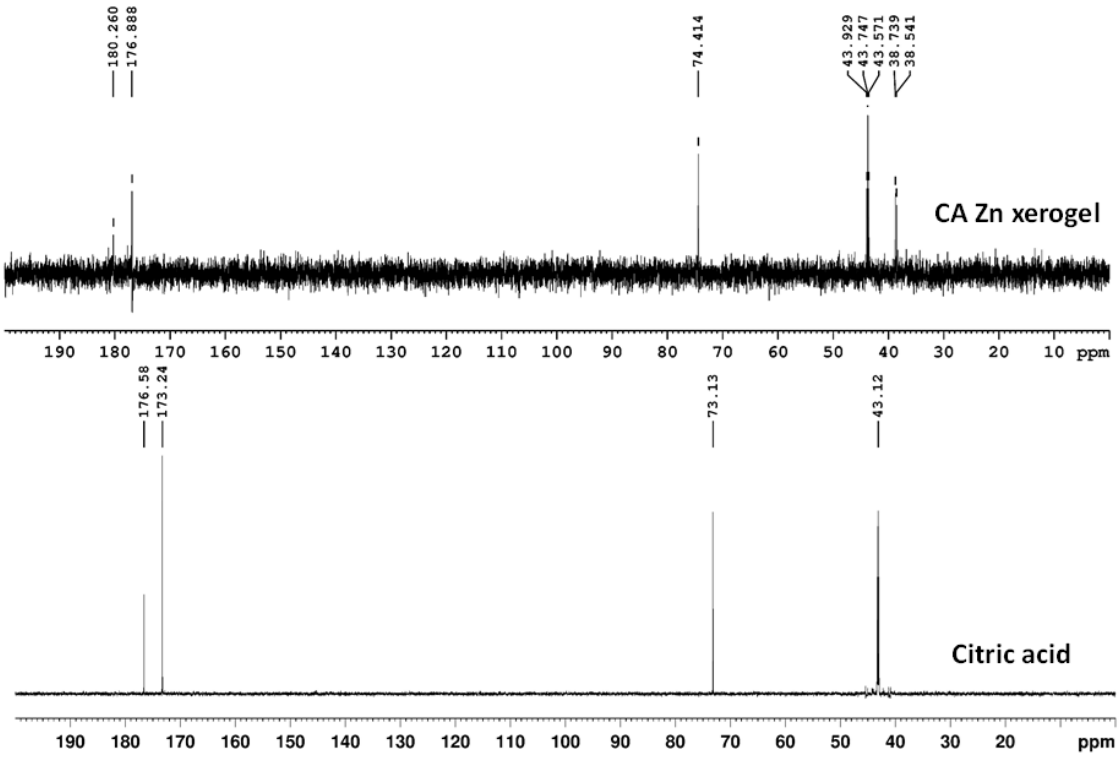

Figure S8: ^{13}C NMR spectra of citric acid and CA Zn xerogel recorded in D_20.

To further confirm the metal-citric acid binding, a similar gel was prepared by mixing citric acid and zinc acetate (1:1 ratio) in DMF and the ^{13}C NMR spectrum of the resultant xerogel is compared with that of uncoordinated citric acid. A significant shift in the peaks corresponding to carboxyl carbons and carbon attached to –OH groups confirms the metal-ligand coordination.

9. Solution state absorption spectra of Tpy with incremental addition of lanthanide ions

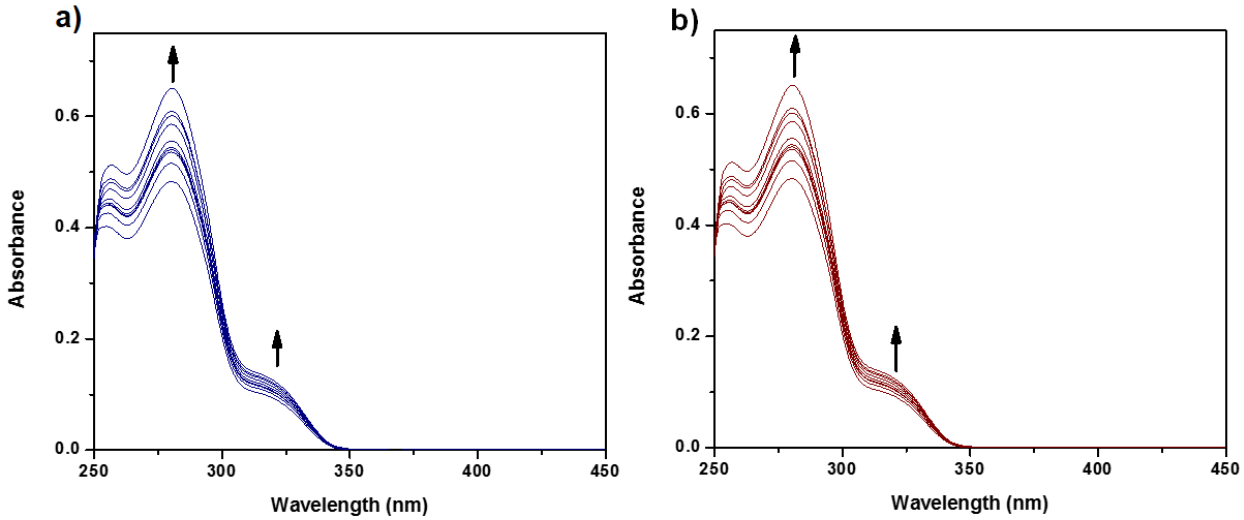

Figure S9: Solution state absorption spectra of Tpy (10^{-5} M) with increasing amounts(0-2 equivalents) of a) Tb (III) ions and b) Eu (III) ions.

10. Luminescence spectra of mixed ligand–lanthanide gels with increasing concentrations of Ln (III) ions

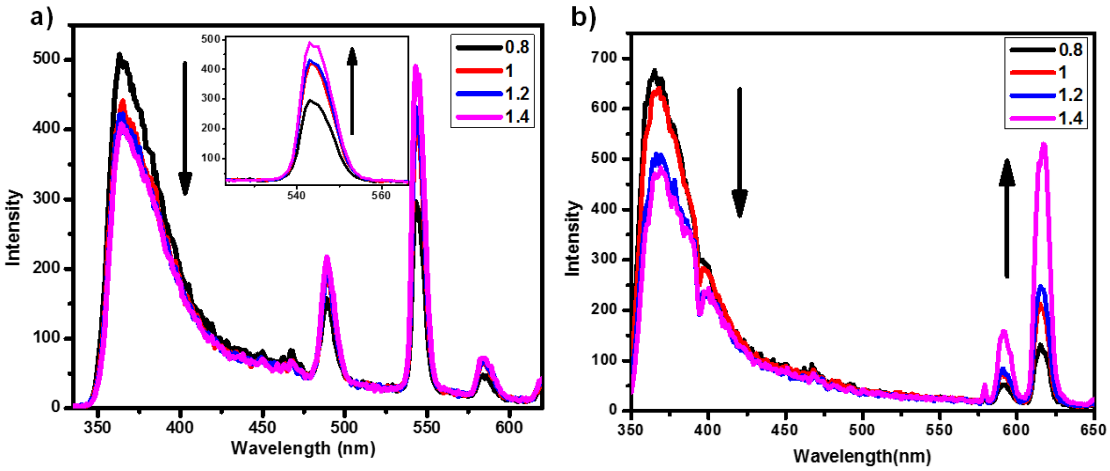

Figure S10: Luminescence spectra of a) CA Tpy Tb with increasing concentrations of Tb (III) ions (0.8-1.4 equivalents) and b) CA Tpy Eu with increasing concentrations of Eu (III) ions (0.8-1.4 equivalents).

11. Theoretical calculation of energy levels

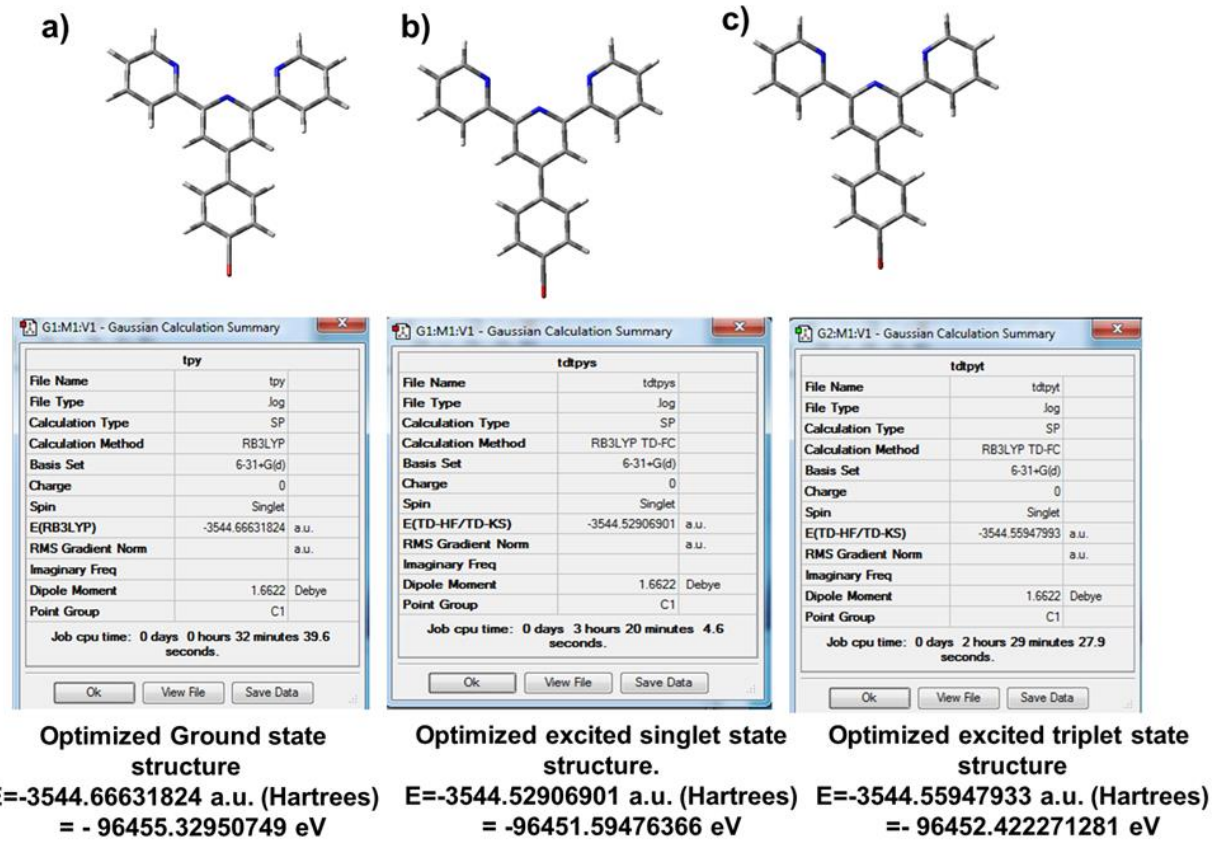

Figure S11: Optimized a) ground, b) singlet, and c) triplet state structure of Tpy obtained by density functional theory calculation with B3LYP/6-31+G(d) theory.

12. Luminescent colour shift of thin film prepared from CA Tpy Tb gel in response to pH verified by CIE chromaticity diagram

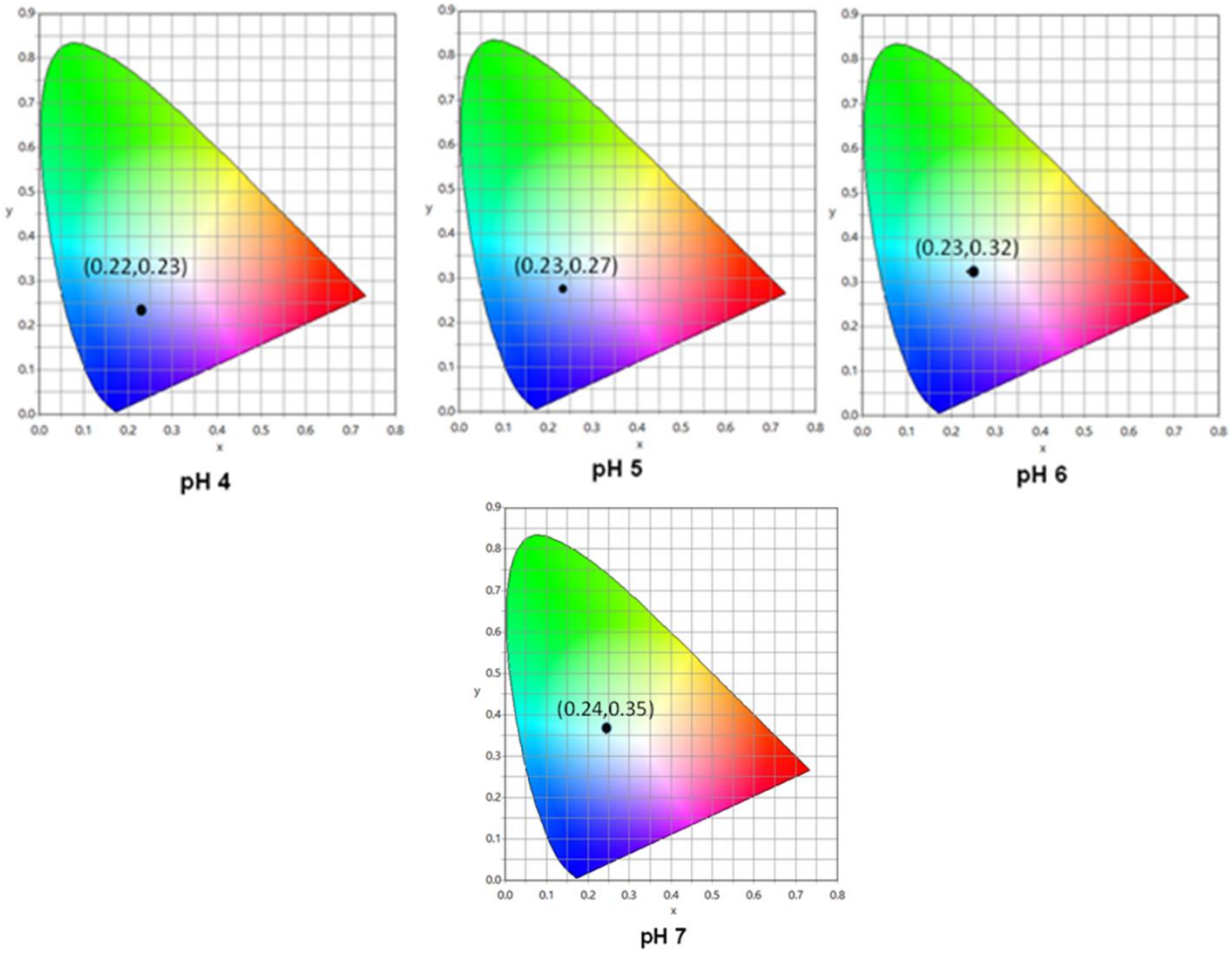

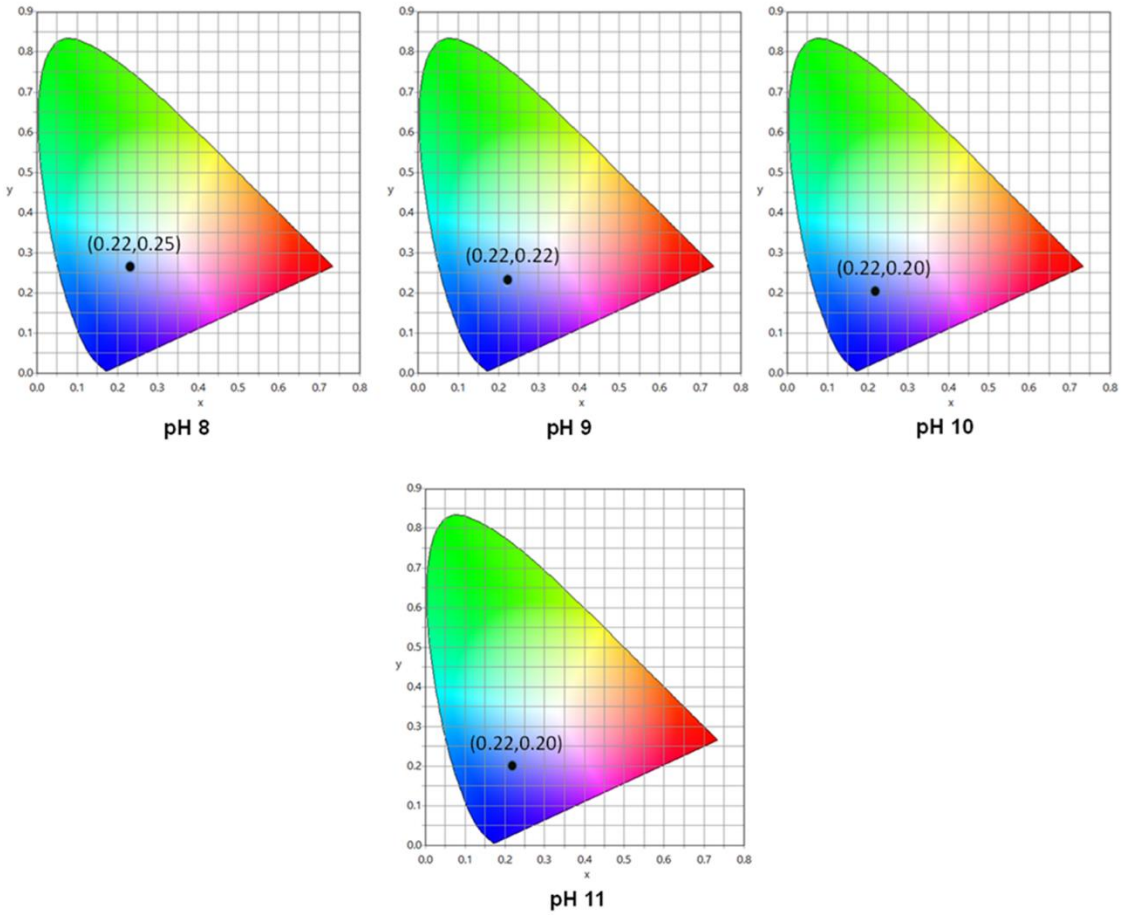

Figure S12: CIE (1931) coordinates diagram for thin film prepared from CA Tpy Tb gel at different pH.

13. Vapor response of thin film prepared from CA Tpy Tb gel.

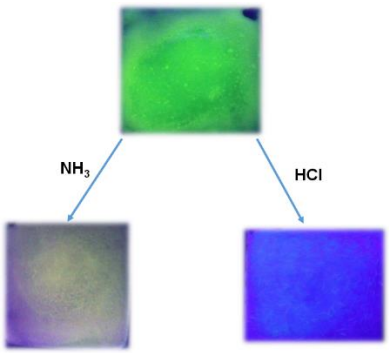

Figure S13: UV illuminated photographs of CA Tpy Tb gel thin film in different vapors.

16. Quantum yield of xerogels

SI No	Gel	Absolute Quantum Yield (%)
1	CA Tpy Tb	4.27
2	CA Tpy Eu	3.87
3	White light emitting gel	3.33

Table S2: Results of absolute quantum yield meassurement of xerogels.

Reference

1. S. G. Liu, W. Liu, J. L. Zuo, Y. Z. Li and X. Z. You, *Inorg. Chem. Commun*., 2005, **8**, 328–330.